

Low Speed Operation of CSI fed Induction Motor Drives with MRAS Based Estimation of Stator Resistance

M.Sivakumar¹, T.Dhanakodi², Dr.N.Panneer Selvam³

^{1,2} Valivalam Desikar Polytechnic College, Nagapattinam Tamilnadu -639 111, India.

³ M.A.M.Polytechnic College Trichirappalli, Tamilnadu-621 105, India.

Abstract

Zero-speed operation can greatly increase the competitive value of the drive and expand its range of applications to include cranes, hoists, and draglines. The performance of vector controlled Sensorless induction motor drives is generally poor at very low speeds, especially at zero speed due to stator resistance variations. The speed estimation is adversely affected by stator resistance variations due to temperature and frequency changes. This is particularly significant at very low speeds where the calculated flux and torque deviates from its set values. Therefore, it is necessary to compensate for the parameter variation in Sensorless induction motor drives, particularly at very low speeds. The performance and efficiency of an induction motor drive system can be enhanced by online estimation of the critical parameters, such as the stator resistance. In This paper proposed a new model reference adaptive system (MRAS)-based algorithm for simultaneous stator resistance (R_s) and rotor speed (ω_r) identification for position Sensorless closed-loop Field oriented vector controlled CSI fed induction motor. The R_s has to be estimated concurrently with the ω estimation to compensate for the fluctuation in R_s . The reference model and adjustable model are interchangeable for concurrent ω and R_s estimation in the low-speed operating region are investigated and simulation results are shown. The simulation results reveal that the proposed method is able to obtain precise flux and torque control, even for very low operating frequencies.

Keywords: Current source inverter, Induction Motor, Sensorless Speed, Resistance tuning, Zero speed

NOMENCLATURE:

C_f	Motor-side filter capacitance.
i_{cd}, i_{cq}	Motor-side capacitor current in the dq reference frame.
i_{dc}, i_{dc}^*	DC-link current and its reference.
$i_s = (i_{\alpha s}, i_{\beta s})^T$	Stator current in the $\alpha\beta$ reference frame.
i_{ds}^*, i_{qs}^*	Stator reference current in the dq reference frame.
i_{dw}^*, i_{qw}^*	Capacitor compensation current in the dq reference frame.

J	Inertia of motor and its load.
K_t	Equivalent torque constant.
L_d	DC-link inductance.
L_m	Magnetizing inductance.
L_s, L_r	Self-inductance of stator and rotor.
T_e	Electromagnetic torque.
T_e^*	Reference Torque
v_{ds}, v_{qs}	Stator voltage in the dq reference frame.
$\Psi_{\alpha s}, \Psi_{\beta s}$	Stator flux linkage in the $\alpha\beta$ reference frame.
Ψ_{ds}, Ψ_{qs}	Stator flux linkage in the dq reference frame.
Ψ_r, Ψ_r^*	Magnitude of rotor flux linkage and its reference.
ω	Motor electrical frequency.
ω_r, ω_r^*	Motor speed and its reference.
σ	Motor total leakage factor.
τ	Time constant of a low-pass filter.
τ_r	Rotor time constant.
θ_f	Angle of rotor flux linkage.
θ	Inverter firing angle.
θ_ω	Angle of inverter reference current.

INTRODUCTION

Simple converter structure, motor-friendly waveforms, inherent four-quadrant operation capability, and reliable short-circuit protection are features that make current-source inverter (CSI) well suited for medium-voltage drives applications [1]-[7]. Vector control strategies are widely employed in the high-power current-source drives to improve the system dynamics and reliability [8].

The concept of vector control for CSI fed high-performance induction motor drive systems has become very popular during the last decades. The induction motor widely used in industries due to low cost and the structure robustness of the machine, this has led to replacement of the direct current machines by induction motors in many applications the last few years [9]–[11]. Several vector control techniques have been proposed, which can be separated into two categories, according to the method used for the flux vector orientation: direct and indirect control schemes. In direct control schemes, the flux vector is calculated using the stator terminal quantities, while indirect methods use the machine slip frequency value to achieve field orientation. However, both methods require the knowledge of machine parameters, which are not precisely known in general. Indirect control schemes require knowledge of the machine inductances as well as the rotor time constant, while in direct schemes only the stator resistance value has to be known for flux estimation. Depending on the specific method, these parameters highly affect the flux vector calculation precision. In past work [12] it has been shown that these parameters vary during operation. Variations can exceed 50% of the startup value. In particular, for the rotor-flux-oriented control method, the stator resistance value is not dominant in the high speed range, so a possible estimation error will not affect the stator flux calculations. In low-speed operation, the stator resistance value becomes critical for the calculations and a stator resistance variation will produce a significant estimation error. An accurate value of the stator resistance is of crucial importance for correct operation of a sensor less drive in the low speed region, since any mismatch between the actual value and the value used within the speed estimator may lead not only to a substantial speed estimation error but to instability as well. As a consequence, numerous on-line schemes for stator resistance estimation have been proposed in recent past [13-18].

In this paper proposes a MRAS based on-line identification of stator resistance and speed estimation for a sensor less rotor-flux-oriented (FOC) vector-controlled CSI fed induction motor drive is presented. The scheme is combines ideas of [17- 19] to propose a simple method for stator on-line resistance identification. Stator resistance estimation is developed in conjunction with the rotor flux based MRAS speed estimator and it operates in the stationary reference frame (in contrast to the schemes of [17, 18]). It does however utilize the idea of [17, 18] related to the creation of the error quantity for adaptive stator resistance identification. The error quantity is formed on the basis of differences in rotor flux component values, obtained at the output of the reference and the adjustable model. The observation of [19], that the role of the reference and the adjustable model is interchangeable for the purposes of speed and stator resistance estimation, is utilized as well. However, in contrast to [19], the operation of the speed and stator resistance estimators is in parallel rather than sequential. This difference is made possible by the observation that the MRAS speed estimator utilizes an error quantity related to instantaneous phase difference between the two estimates of the rotor flux. The same error quantity was used in [19] for stator resistance estimation, while the second degree of freedom, the difference in amplitudes of two rotor

flux estimates, was not utilized. This difference is used in this paper as the basis for stator resistance identification. A detailed derivation of the parallel rotor speed and stator resistance estimation algorithms is provided in the paper and the proposed scheme is verified by MATLAB/SIMULINK software. Accurate stator resistance estimation is achieved below 0.5 Hz frequency of rotation.

CURRENT SOURCE DRIVE SYSTEM AND ITS CONTROL SCHEME

Fig.1 illustrates the block diagram of a current source drive system and its FOC control scheme. The current source drive consists of an input LC filter, a PWM CSR, a dc link choke, a PWM CSI and an output filter capacitor. A high power induction motor is connected at the output of the drive. A single-bridge configuration is usually used for both the rectifier and the inverter, with which the drive system can be used for medium voltage applications by connecting switching devices in series in each converter phase leg. The drive's input and output filter capacitors are required to assist the commutation of switching devices, while they can also attenuate unwanted harmonics. The dc choke between the CSR and CSI is used to smooth the dc current. It also prevents the dc current from sudden increase in case of short-circuit fault and thus provides sufficient time for the protection circuit to function. The FOC scheme for the current source drive system is based on the rotor flux orientation and the decoupled control of the motor flux and torque provides improved dynamics and stability. For the rotor flux estimation, voltage model rotor flux identification method (using the motor stator voltage and current) combined with current model method (using the stator current and the rotor speed) is implemented for an optimal system performance. The current model method can estimate the rotor flux precisely at low rotor speeds with the stator frequency of a few Hertz.

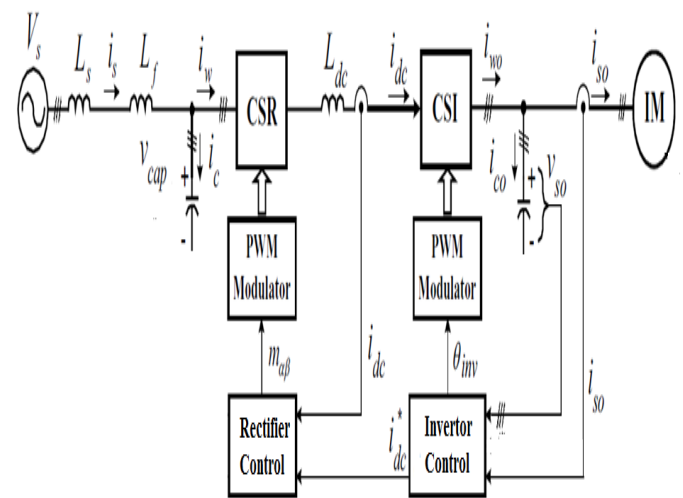


Figure 1. Field oriented control Current source inverter drive system

BASIC SPEED ESTIMATOR AND VECTOR CONTROL SCHEME

In this paper to analyze the speed estimator is originally proposed in [20] and illustrated in Fig. 2, where the two left-hand side blocks perform integration of equations (1) and (2). The reference (voltage) model and adjustable (current) models are derived by the stator voltage and currents. The estimator operates in the stationary reference frame (α), and it is described with the following equations [20]:

$$p \underline{\hat{\Psi}}_{rV}^s = \frac{L_m}{L_r} [\underline{u}_s^s - (\hat{R}_s + \sigma L_s p) \underline{i}_s^s] \quad (1)$$

$$p \underline{\hat{\Psi}}_{rI}^s = \frac{L_m}{T_r} \underline{i}_s^s - \left(\frac{1}{T_r} - j\hat{\omega} \right) \underline{\hat{\Psi}}_{rI}^s \quad (2)$$

$$\hat{\omega} = \left(K_p \omega + \frac{K_{I\omega}}{p} \right) e_\omega \quad (3)$$

$$e_\omega = \underline{\hat{\Psi}}_{rI}^s \times \underline{\hat{\Psi}}_{rV}^s = \hat{\Psi}_{\alpha r I}^s \hat{\Psi}_{\beta r V}^s - \hat{\Psi}_{\beta r I}^s \hat{\Psi}_{\alpha r V}^s \quad (4)$$

A symbol $\hat{}$ denotes in (1) - (4) estimated quantities, symbol 'p' stands for d/dt , T_r is the rotor time constant and $\sigma = 1 - L_m^2/L_s L_r$. All the parameters in the motor and the estimator are assumed to be of the same value, except for the stator resistance (hence a hat above the symbol in (1)). Underlined variables are space vectors, and sub-scripts V and I stand for the outputs of the voltage (reference) and current (adjustable) models, respectively. Voltage, current and flux are denoted with u , i and ψ , respectively, and subscripts s and r stand for stator and rotor, respectively. Superscript s in space vector symbols denotes the stationary reference frame.

As is evident from (1)-(4) and Fig. 2, the adaptive mechanism (PI controller) relies on an error quantity that represents the difference between the instantaneous positions of the two rotor flux estimates. The second degree of freedom, the difference in amplitudes of the two rotor flux estimates, is not utilized. The parallel rotor speed and stator resistance MRAS estimation scheme, which will be developed in the next section, will make use of this second degree of freedom to achieve simultaneous estimation of the two quantities. The role of the reference and the adjustable model will be interchanged for this purpose, since the rotor flux estimate of (2) is independent of stator resistance.

The rotor flux oriented control scheme for an induction motor, utilized in the paper in simulation is illustrated in Fig. 3. It includes, apart from a speed controller, rotor flux and torque controllers as well. The required feedback quantities for the torque and rotor flux closed loop control are obtained from the reference model (1). Induction motor data are given in the Appendix.

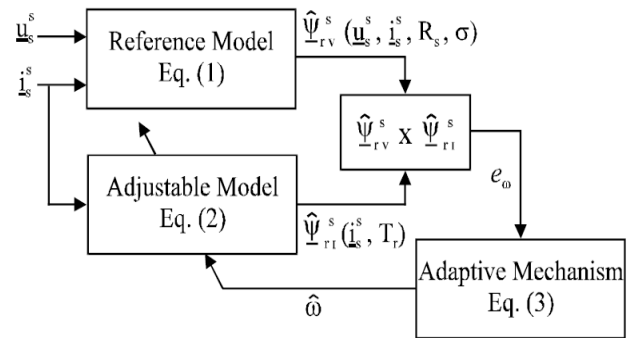


Figure 2. Basic configuration of the rotor flux based MRAS speed estimator

The induction motor control scheme is shown in Fig. 3, where rotor flux orientation is employed [20]. The flux and speed controllers are utilized to generate the motor d -axis current (i_{ds}^*) and q -axis current (i_{qs}^*), respectively. The sum of stator d , q -axis currents and the compensated capacitor currents is used to produce the inverter reference d , q -axis currents (i_{dw}^* and i_{qw}^*). In order to minimize the dc-link current, the amplitude (i_{dc}^*) of the synthesized inverter reference current is served as the reference for dc-link current control of the current source rectifier, while the corresponding phase θ_w is added to the rotor flux angle θ_f for the modulation of the CSI. The current model is utilized for the flux estimation

IMPACT OF FILTER CAPACITOR ON SYSTEM CONTROL

CSI-fed motor drives have filter capacitors connected at the output of the inverter. This means that a portion of the inverter currents go through the capacitors. The influence of the filter capacitors on the system control is investigated in this section. The inverter reference currents can be expressed as follows [20]:

$$\begin{aligned} i_{dw}^* &= i_{cd} + i_{ds}^* \\ i_{qw}^* &= i_{cq} + i_{qs}^* \end{aligned} \quad (5)$$

where i_{cd} and i_{cq} are the estimated capacitor d , q -axis currents. To reduce the sensitivity and noise caused by the derivative terms, the estimated capacitor currents are usually simplified as follows:

$$\begin{aligned} i_{cd} &= -\omega_e v_{qs} C_f \\ i_{cq} &= \omega_e v_{ds} C_f \end{aligned} \quad (5a)$$

Where C_f , ω_e , v_{ds} , and v_{qs} are the inverter-side filter capacitance, motor electrical angular frequency, and stator d -axis and q -axis voltages, respectively.

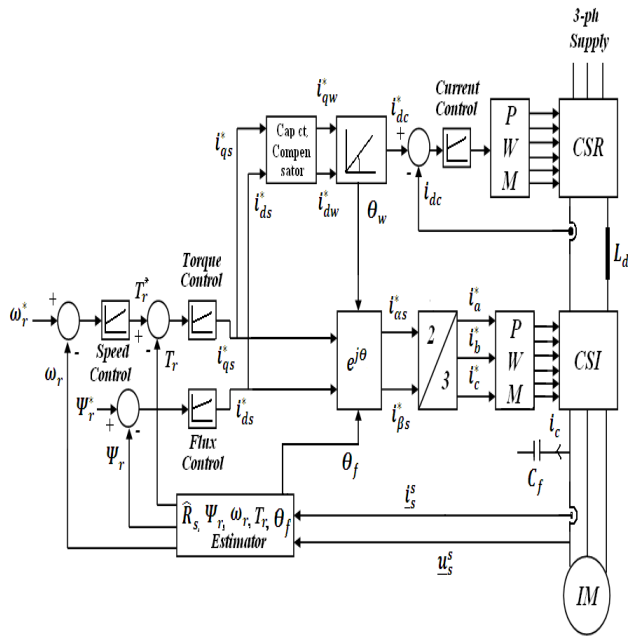


Figure 3. Structure of the speed sensor less current-fed rotor flux oriented induction motor drive

PARALLEL STATOR RESISTANCE AND ROTOR SPEED ESTIMATION

Proposed parallel rotor speed and stator resistance estimation scheme is designed based on the concept of hyper stability [20] in order to make the system asymptotically stable. For the purpose of deriving an adaptation mechanism it is valid to initially treat rotor speed as a constant parameter, since it changes slowly compared to the change in rotor flux. The stator resistance of the motor varies with temperature, but variations are slow so that it can be treated as a constant parameter, too. The configuration of the proposed parallel rotor speed and stator resistance is shown in Fig. 4 and is discussed in detail next.

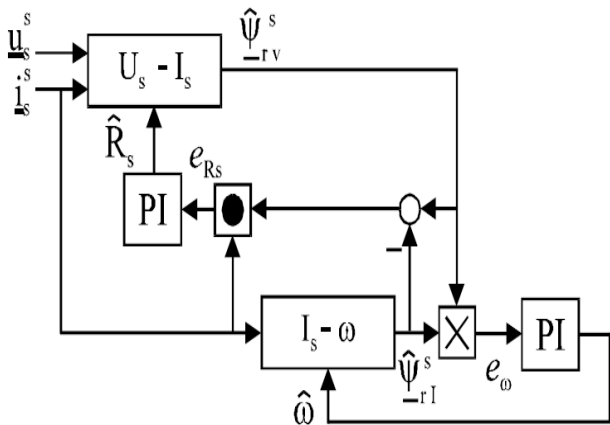


Figure 4. Structure of the MRAS system for parallel rotor speed and stator resistance estimation.

Let R_s and ω_r denote the true values of the stator resistance in the motor and rotor speed, respectively. These are in general different from the estimated values. Consequently, a mismatch between the estimated and true rotor flux space vectors appears as well. The error equations for the voltage and the current model outputs can then be written as

$$p \underline{\varepsilon}_V = -\frac{L_r}{L_m} (R_s - \hat{R}_s) \underline{i}_s^s \quad (6a)$$

$$\underline{\varepsilon}_V = \underline{\Psi}_{rV}^s - \hat{\underline{\Psi}}_{rV}^s = \varepsilon_{\alpha V} + j \varepsilon_{\beta V} \quad (6b)$$

$$p \underline{\varepsilon}_I = \left(j\omega - \frac{1}{T_r} \right) \underline{\varepsilon}_I + j(\omega - \hat{\omega}) \hat{\underline{\Psi}}_{rI}^s \quad (6c)$$

$$\underline{\varepsilon}_I = \underline{\Psi}_{rI}^s - \hat{\underline{\Psi}}_{rI}^s = \varepsilon_{\alpha I} + j \varepsilon_{\beta I} \quad (6d)$$

Symbols $\underline{\Psi}_{rV}^s, \underline{\Psi}_{rI}^s$ in (6b), (6b) stand for true values of the two rotors flux space vectors. Equations (6a)-(6d) can be rewritten in matrix notation as

$$p \begin{bmatrix} \varepsilon_{\alpha I} \\ \varepsilon_{\beta I} \\ \varepsilon_{\alpha V} \\ \varepsilon_{\beta V} \end{bmatrix} = \begin{bmatrix} -\frac{1}{T_r} & -\omega & 0 & 0 \\ \omega & -\frac{1}{T_r} & 0 & 0 \\ 0 & 0 & 0 & 0 \\ 0 & 0 & 0 & 0 \end{bmatrix} \begin{bmatrix} \varepsilon_{\alpha I} \\ \varepsilon_{\beta I} \\ \varepsilon_{\alpha V} \\ \varepsilon_{\beta V} \end{bmatrix} - W = A \underline{\varepsilon} - W \quad (7)$$

Where W is the nonlinear block, defined as follows:

$$W = \begin{bmatrix} -\Delta\omega \begin{bmatrix} 0 & -1 \\ 1 & 0 \end{bmatrix} & 0 & 0 \\ 0 & 0 & \frac{L_r}{L_m} \Delta R_s \begin{bmatrix} 1 & 0 \\ 0 & 1 \end{bmatrix} \end{bmatrix} \begin{bmatrix} \hat{\Psi}_{\alpha r I}^s \\ \hat{\Psi}_{\beta r I}^s \\ i_{\alpha s}^s \\ i_{\beta s}^s \end{bmatrix} \quad (8)$$

$$W = \begin{bmatrix} -\Delta\omega j & 0 \\ 0 & \frac{L_r}{L_m} \Delta R_s I \end{bmatrix} \cdot \begin{bmatrix} \hat{\Psi}_{r I}^s \\ i_s^s \end{bmatrix}$$

Here $\Delta\omega = \omega - \hat{\omega}$,

$$\Delta R = R_s - \hat{R}_s \quad \Psi_{r I}^s = [\hat{\Psi}_{\alpha r I}^s \quad \hat{\Psi}_{\beta r I}^s]^T,$$

$$i_s^s = [i_{\alpha s}^s \quad i_{\beta s}^s]^T, \quad J = \begin{bmatrix} 0 & -1 \\ 1 & 0 \end{bmatrix}$$

$$\text{and } I = \begin{bmatrix} 1 & 0 \\ 0 & 1 \end{bmatrix}$$

The system is hyper stable if the input and output of the nonlinear block W satisfy Popov's criterion [20]:

$$S = \int_0^{t_1} \underline{\varepsilon}^T \cdot W dt \geq \gamma^2 \cdot \forall t_1 \quad (9)$$

Where, using (8)

$$\underline{\varepsilon}^T \cdot W = -\Delta\omega(\underline{\varepsilon}_i^T \cdot J \cdot \hat{\Psi}_{r1}^s) + \frac{L_r}{L_m} \Delta R_s(\underline{\varepsilon}_v^T \cdot i_s^s) \quad (10)$$

Substitution of (10) into (9) yields

$$S = \int_0^{t_1} \underline{\varepsilon}^T \cdot W dt = - \underbrace{\int_0^{t_1} \Delta\omega(\underline{\varepsilon}_i^T \cdot J \cdot \hat{\Psi}_{r1}^s) dt}_{S_1} + \underbrace{\frac{L_r}{L_m} \int_0^{t_1} \Delta R_s(\underline{\varepsilon}_v^T \cdot i_s^s) dt}_{S_2}$$

$$s = S_1 + \frac{L_r}{L_m} \cdot S_2 \geq -\gamma^2 \cdot \forall t_1 \quad (11)$$

The validity of (11) can be verified by means of inequalities (12) and (13) with adaptive mechanisms given in (14), (15) for rotor speed estimation and stator resistance identification, respectively:

$$S_1 = - \int_0^{t_1} \Delta\omega(\underline{\varepsilon}_i^T \cdot J \cdot \hat{\Psi}_{r1}^s) dt \geq -\gamma_1^2 \quad (12)$$

$$S_2 = \int_0^{t_1} \Delta R_s(\underline{\varepsilon}_v^T \cdot i_s^s) dt \geq -\gamma_2^2 \quad (13)$$

$$\hat{\omega} = \left(K_{p\omega} + \frac{K_{i\omega}}{p} \right) (\underline{\varepsilon}_i^T \cdot J \cdot \hat{\Psi}_{r1}^s) = \left(K_{p\omega} + \frac{K_{i\omega}}{p} \right) e_{\omega} \quad (14)$$

$$\hat{R}_s = \left(K_{pR_s} + \frac{K_{iR_s}}{p} \right) (\underline{\varepsilon}_v^T \cdot i_s^s) = \left(K_{pR_s} + \frac{K_{iR_s}}{p} \right) e_{R_s} \quad (15)$$

Where $K_{p\omega}$, $K_{i\omega}$, K_{pR_s} , K_{iR_s} , are PI controller parameters of rotor speed and stator resistance adaptation mechanisms, respectively. The value of $\underline{\varepsilon}_i^T \cdot J \cdot \hat{\Psi}_{r1}^s$ in (12), (14) is evaluated by taking into account that, for speed estimation, the output of the reference model (1) is taken as equal to the true rotor flux space vector. Hence $\underline{\varepsilon}_1 = \underline{\Psi}_{r1}^s - \hat{\Psi}_{r1}^s = \underline{\Psi}_{rv}^s - \hat{\Psi}_{r1}^s$, since $\underline{\Psi}_{r1}^s \equiv \hat{\Psi}_{rv}^s$, Thus

$$\underline{\varepsilon}_i^T \cdot J \cdot \hat{\Psi}_{r1}^s = [\hat{\Psi}_{arv} - \hat{\Psi}_{ar1} \quad \hat{\Psi}_{\beta r1} - \hat{\Psi}_{\beta rv}] \cdot \begin{bmatrix} 0 & -1 \\ 1 & 0 \end{bmatrix} \cdot \begin{bmatrix} \hat{\Psi}_{ar1} \\ \hat{\Psi}_{\beta r1} \end{bmatrix}$$

$$= [\hat{\Psi}_{arv} - \hat{\Psi}_{ar1} \quad \hat{\Psi}_{\beta r1} - \hat{\Psi}_{\beta rv}] \cdot \begin{bmatrix} -\hat{\Psi}_{\beta r1} \\ \hat{\Psi}_{ar1} \end{bmatrix}$$

$$= \hat{\Psi}_{r1}^s \hat{\Psi}_{rv}^s = e_{\omega}(t) \quad (16)$$

The error quantity for speed estimation is therefore the one of (4). The value of $\underline{\varepsilon}_v^T \cdot i_s^s$ in (13), (15) needs to be evaluated next. In order to do this, it is necessary to take into account that, for stator resistance estimation, reference and adjustable model (1), (2) change the roles. The true value of the rotor flux space vector is now taken to be the output of (2). Hence $\underline{\varepsilon}_v = \underline{\Psi}_{rv}^s - \hat{\Psi}_{rv}^s = \hat{\Psi}_{r1}^s - \underline{\Psi}_{rv}^s$, since $\underline{\Psi}_{rv}^s \equiv \hat{\Psi}_{r1}^s$.

One further has

$$-\underline{\varepsilon}_v^T \cdot i_s^s = [\hat{\Psi}_{arv} - \hat{\Psi}_{ar1} \quad \hat{\Psi}_{\beta rv} - \hat{\Psi}_{\beta r1}] \cdot \begin{bmatrix} \hat{\Psi}_{ar1} \\ \hat{\Psi}_{\beta r1} \end{bmatrix}$$

$$= i_{as}(\hat{\Psi}_{arv} - \hat{\Psi}_{ar1}) + i_{\beta s}(\hat{\Psi}_{\beta rv} - \hat{\Psi}_{\beta r1})$$

$$= i_s^s(\underline{\Psi}_{rv} - \underline{\Psi}_{r1}) = e_{R_s}(t) \quad (17)$$

The error quantity for stator resistance estimation is therefore

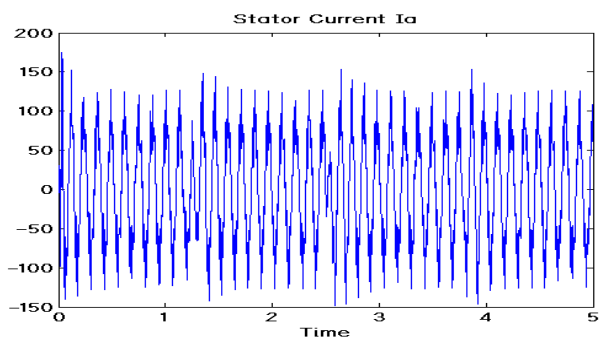
$$e_{R_s} = i_{as}(\hat{\Psi}_{arv} - \hat{\Psi}_{ar1}) + i_{\beta s}(\hat{\Psi}_{\beta rv} - \hat{\Psi}_{\beta r1}) \quad (18)$$

It follows from these considerations that the role of the reference and the adjustable models is interchangeable in the parallel system of rotor speed and stator resistance estimation. The speed and stator resistance can be estimated in parallel using (14), (15) at any speed. The rotor speed adaptation mechanism (14) is the same as in the customary MRAS speed estimator reviewed in Section II. Stator resistance adaptation mechanism (15) is, at the first sight, similar to the one of [17, 18]. However, stator resistance is here estimated in the stationary reference frame (rather than in the rotor flux oriented reference frame), and error quantity is obtained using two rotor flux space vector estimates (rather than the reference and a single estimated value, as in [18]). Further, stator resistance and rotor speed estimation operate in parallel, rather than sequentially as in [19]. This is enabled by utilizing the second available degree of freedom (the difference in rotor flux amplitudes) in the process of stator resistance estimation.

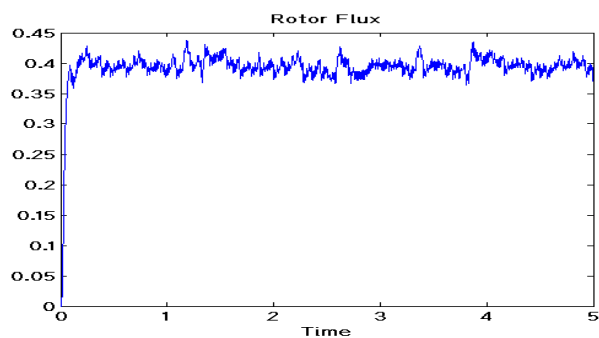
VERIFICATION OF THE PARALLEL ESTIMATION SCHEME

A. Simulation Results

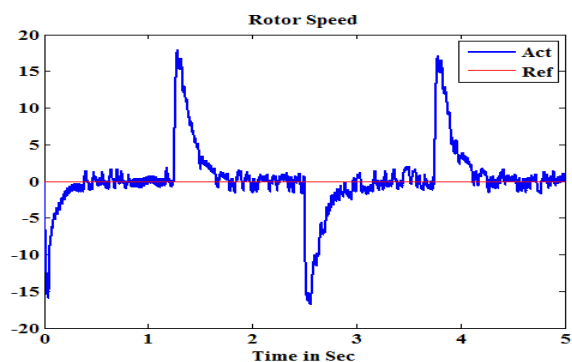
A sample of simulation results is presented here. The presented simulation results in Figs.5 and 6 were made using MATLAB and Simulink software package to show the influence of MRAS controller with and without stator resistance tuning respectively. The sensor less FOC controlled CSI fed with MRAS controller induction motor drive, shown in Fig. 3, is started under load conditions, with the stator resistance estimator turned off. The actual stator resistance in the motor is taken as nominal motor resistance R_s , while the value in the estimator in Fig. 2 is set to the nominal value. The simulation results of the presented control system MRAS with and without stator resistance tuning is shown in fig (5) and (6) respectively. The low speed performance evaluated at zero speed operation with fast load changes. The actual and reference speed, torque stator current and rotor flux are presented in fig 5 and 6. The estimation error is very small in steady state and becomes higher at point of load changes. From the fig 6 the results prove that the performance of simultaneously speed estimation and stator resistance tuning are improved



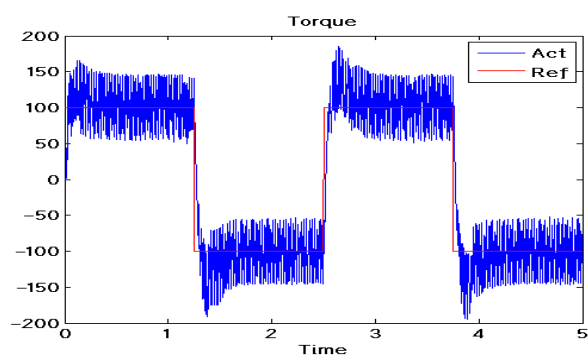
(a)



(b)

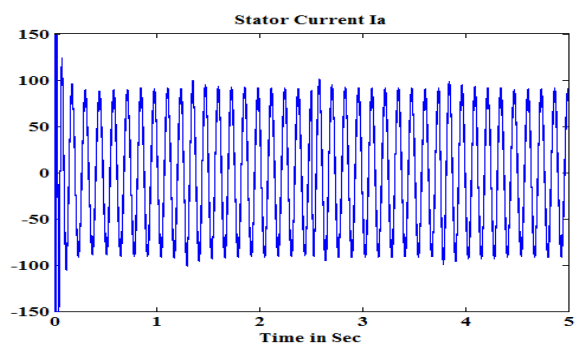


(c)

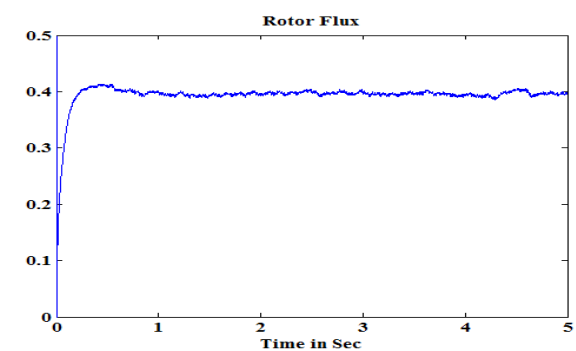


(d)

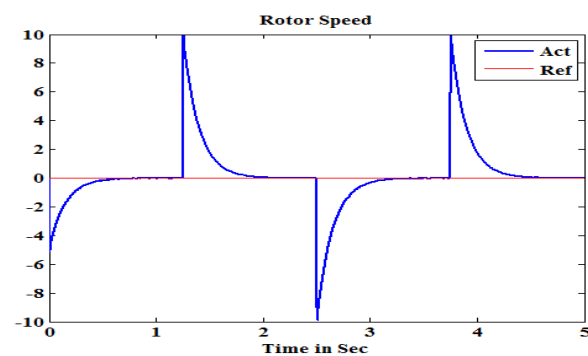
Figure 5. Simulation results for MRAS without R_s Tuning. (a) Stator Current, (b) Rotor Flux, (c) Rotor Speed in RPM, (d) Electromagnetic Torque in NM



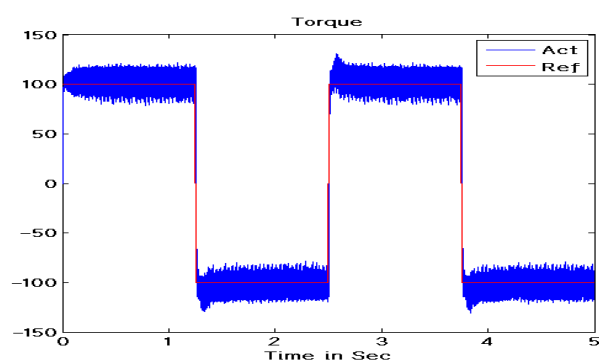
(a)



(b)



(c)



(d)

Figure 6. Simulation results for MRAS with R_s Tuning. (a) Stator Current, (b) Rotor Flux, (c) Rotor Speed in RPM, (d) Electromagnetic Torque in NM

A. Experimental Results:

A experimental system is constructed for experimental verification with key parameters listed in Appendix. A dc motor is coupled to the shaft of the induction machine. It is supplied by a brushless dc motor drive to generate the step load torque. Experiments were obtained using a DSP TMS320C32 from Texas Instruments Incorporated. Connection to the peripherals and signal unit is made with an FPGA. All measured and controller internal variables are accessible through the serial link to the PC, where graphical data-analysis software can be run. The sampling time of the measurements and computation of control algorithm are both 200 μ s. A brushless ac servomotor mechanically connected to the IM under test was used as the load machine. The control of both speed and applied torque is possible, thus, a hardware-in-the-loop operation can also be performed (Fig. 7). The performance of the presented control system with Sensorless speed with paralleling stator resistance tuning by MRAS controlled drives is shown with zero-speed operation with fast load changes (Fig. 8).

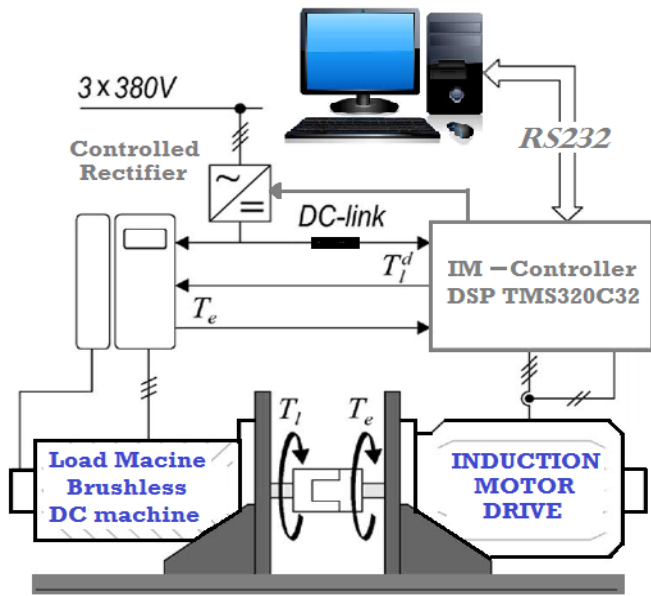
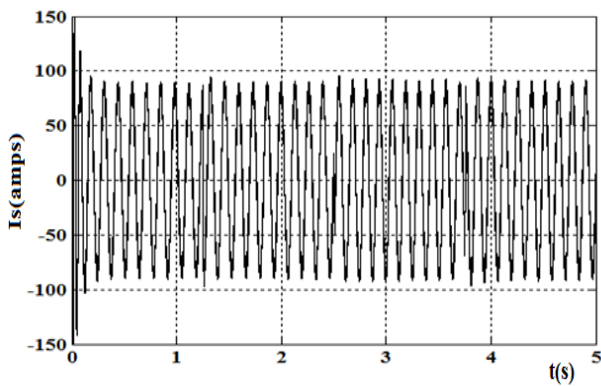
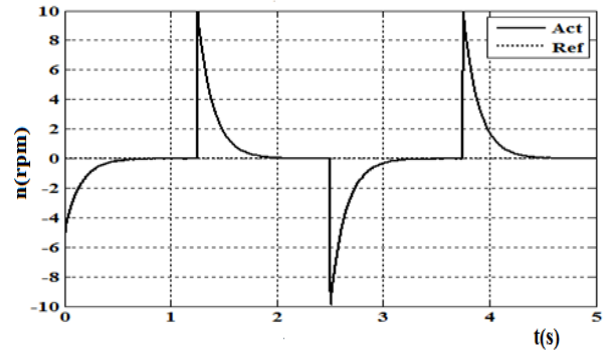


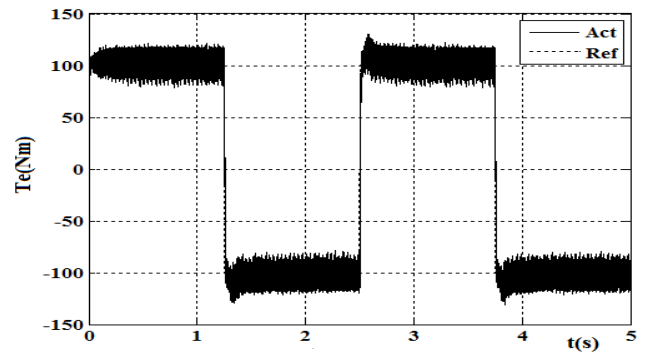
Figure 7. Experimental system



(a)



(b)



(c)

Figure 8. Zero Speed operation
 (a) Stator Current, (b) Reference and actual rotor speed
 (c) Reference and actual load torque

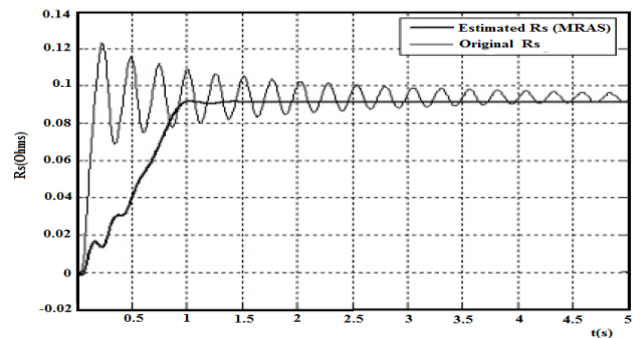


Figure 9. Estimated Stator Resistance

The low-speed performance can be evaluated at zero speed operation with fast load changes. The stator current, actual and estimated speeds are presented in Fig. 8(b). Load changes are presented in Fig. 8(c). Estimation error is very small in steady state and becomes higher at points of load changes, which occur very fast. Otherwise, zero speed is holding satisfactorily. The applied torque of the load machine is measured, and thus, the value of the torque applied by the drive machine is obtained. Actual values of load torque as well as reference values of torque obtained by the speed controller are presented in Fig. 8. It can be seen that the desired torque matches the load torque in steady state. Figure

9 shows the actual and estimated stator resistance of machine with MRAS. The MRAS estimator is able to estimate the resistance value during the low speed operation.

CONCLUSIONS:

The paper presents a parallel MRAS estimator that enables simultaneous estimation of rotor speed and stator resistance. The proposed method has been applied to CSI fed FOC induction motor drive without speed sensor. The parallel adaptive approach is used to identify R_s to enhance the robustness of the Sensorless induction motor drive in the range of low speed. The proposed estimator can estimate the stator resistance over a wide range resistance variation due to temperature and frequency changes. The structure of the estimator is derived using hyper stability theory and it utilizes both degrees of freedom, available within the standard rotor flux based MRAS speed estimator. The error in the instantaneous phase position of the two rotor flux estimates is utilized for rotor speed identification, this being the same as in the standard approach. The second degree of freedom, the error in the amplitudes of the two rotor flux estimates, is used for parallel stator resistance estimation. The proposed parallel MRAS system is insignificantly more complex than its counterpart with speed estimation only and it enables very good speed estimation accuracy down to very low speeds or zero speed. The effectiveness of the developed parallel MRAS structure is verified by simulation and experimental at low-speed region. The proposed estimator can estimate the stator resistance over wide range resistance variations due to temperature and frequency changes. The estimation error of speed and stator resistance is very small and the speed response is adequate for variable speed drives. The capability of the drive to operate at zero speed and the simulation and experimental results show that the CSI fed FOC induction motor with MRAS controller with stator resistance tuning works well at zero speed with promising the good speed performance.

APPENTIX

Induction motor parameters

Rated Power	50 hp
Rated Voltage	460 V
Stator Resistance	0.087 Ω
Rotor Resistance	0.228 Ω
Stator Inductance	35.5 mH
Rotor Inductance	35.5 mH
Mutual Inductance	34.7 mH
Moment of inertia	1.662 kg.m ²
Friction co efficient	0.1 N.m.s/rad
Number of poles	4
Line side Capacitor	500 μ F
Inverter side Capacitor	500 μ F
DC inductance	35mH

REFERENCES

- [1] Y.W. Li, M. Pande, N. R. Zargari, and B.Wu, "Dc-link current minimization for high-power current-source motor drives," *IEEE Trans. Power Electron.*, vol. 24, no. 1, pp. 232–240, Jan. 2009.
- [2] Weber, P. Kern, and T. Dalibor, "A novel 6.5 kV IGCT for high power current source inverters," in *Proc. Int. Symp. Power Semicond. Devices ICs*, Osaka, Japan, 2001, pp. 215–218.
- [3] N.R. Zargari, S.C.Rizzo, Y.Xiao, H. Iwamoto, K. Satoh, and J. F. Donlon, "A new current-source converter using a symmetric gate-commutated thyristor (SGCT)," *IEEE Trans. Ind. Appl.*, vol. 37, no. 3, pp. 896–903, May/June. 2001.
- [4] Y. W. Li, M. Pande, N. R. Zargari, and B. Wu, "An input power factor control strategy for high-power current-source induction motor drive with active front-end," *IEEE Trans. Power Electron.*, vol. 25, no. 2, pp. 352–359, Feb. 2010.
- [5] J.D.Ma, B.Wu, N. R. Zargari, and S. C. Rizzo, "A space vector modulated CSI-based ac drive for multi motor applications," *IEEE Trans. Power Electron.*, vol. 16, no. 4, pp. 535–544, Jul. 2001.
- [6] A.Klonne and F.W. Fuchs, "High dynamic performance of a PWM current source converter induction machine drive," in *Proc. 10th Eur. Conf. Power Electron. Appl.*, 2003, pp. 1–10.
- [7] V. D. Colli, P. Cancelliere, F. Marignetti, and R. D. Stefano, "Influence of voltage and current source inverters on low-power induction motors," *IEE Proc. Electr. Power Appl.*, vol. 152, no. 5, pp. 1311–1320, Sep. 2005.
- [8] M. Salo and H. Tuusa, "A vector-controlled PWM current-source-inverter fed induction motor drive with a new stator current control method," *IEEE Trans. Ind. Electron.*, vol. 52, no. 2, pp. 523–531, Apr. 2005.
- [9] G. O. Garcia, R. M. Stephan, and E. H. Watanabe, "Comparing the indirect field-oriented control with a scalar method," *IEEE Trans. Ind. Electron.*, vol. 41, pp. 201–207, Apr. 1994.
- [10] M. P. Kazmierkowski and A. B. Kasprowicz, "Improved direct torque and flux vector control of PWM inverter-fed induction motor drives," *IEEE Trans. Ind. Electron.*, vol. 42, pp. 344–350, Aug. 1995.
- [11] Y. T. Kao and C. H. Liu, "Analysis and design of microprocessor-based vector-controlled induction motor drives," *IEEE Trans. Ind. Electron.*, vol. 39, pp. 46–54, Feb. 1992.
- [12] R. Marino, S. Peresada, and P. Tomei, "On-line stator and rotor resistance estimation for induction motors," *IEEE Trans. Contr. Syst. Technol.*, vol. 8, pp. 570–579, May 2000.

- [13] L. Umanand, and S. R. Bhat, "Online estimation of stator resistance of an induction motor for speed control applications," *IEE Proc. – Electric Power Applications*, vol. 142, no. 2, pp. 97-103, 1995.
- [14] R. J. Kerkman, B. J. Seibel, T. M. Rowan, and D. Schlegel, "A new flux and stator resistance identifier for ac drive systems," *IEEE Trans. On Industry Applications*, vol. 32, no. 3, pp. 585-593, 1996.
- [15] T. G. Habetler, F. Profumo, G. Griva, M. Pastorelli, and A. Bettini, "Stator resistance tuning in a stator-flux field-oriented drive using an instantaneous hybrid flux estimator," *IEEE Trans. on Power Electronics*, vol. 13, no. 1, pp. 125-133, 1998.
- [16] I.J.Ha, and S.H.Lee, "An online identification method for both stator and rotor resistance of induction motors without rotational transducers," *IEEE Trans. on Industrial Electronics*, vol. 47, no. 4, pp. 842-853, 2000.
- [17] M. Tsuji, S. Chen, K. Izumi, and E. Yamada, "A sensorless vector control system for induction motors using q-axis flux with stator resistance identification," *IEEE Trans. on Industrial Electronics*, vol. 48, no. 1, pp. 185-194, 2001.
- [18] K.Akatsu, and A.Kawamura, "Sensorless very low-speed and zero-speed estimations with online rotor resistance estimation of induction motor without signal injection," *IEEE Trans. on Industry Applications*, vol. 36, no. 3, pp. 764-771, 2000.
- [19] L.Zhen, and L.Xu, "Sensorless field orientation control of induction machines based on a mutual MRAS scheme," *IEEE Trans. on Industrial Electronics*, vol. 45, no. 5, pp. 824-831, 1998.
- [20] C.Schauder, "Adaptive speed identification for vector control of induction motors without rotational transducers," *IEEE Trans. On Industry Applications*, vol. 28, no. 5, pp. 1054-1061, 1992.